

# Factorization of the $Q^2$ dependence in electroproduction of vector mesons

E. Ferreira

*Instituto de Física, Universidade Federal do Rio de Janeiro*

*C.P. 68528, Rio de Janeiro 21945-970, RJ, Brazil*

V.L. Baltar

*Departamento de Física, Pontifícia Universidade Católica do Rio de Janeiro*

*C.P. 38071, Rio de Janeiro 22452-970, RJ, Brazil*

## Abstract

In a framework for nonperturbative QCD calculation of high energy processes, the amplitudes for photo- and electroproduction of vector mesons are written as integrals of the overlap product of photon and vector meson wave functions, multiplied by the amplitude for the scattering of  $q\bar{q}$  dipole pairs off the proton. For sizes of the overlap functions that are smaller than the typical ranges of the interaction of the dipoles with the proton, the amplitudes factorize in the form of integrals, here called overlap strengths, formed only with the overlap of the wave functions times the square of the dipole separation. The integration is extended over the light front coordinates describing the  $q\bar{q}$  dipoles. With this result, the overlap strengths contain all  $Q^2$  dependence of the observables. We show the importance of this factorization in the description of the experimental data for all S-wave vector mesons.

## I. INTRODUCTION

In nonperturbative treatments of elastic photo and electroproduction of vector mesons [1, 2, 3] the photon and vector meson wave functions appear as explicit ingredients of the calculation, with an overlap product formed to describe the transition from real or virtual photon to the final meson state. The photon and vector meson are treated in a simple dipole model of quark-antiquark distribution functions, which is responsible for the hadronic character of the interaction with the proton. On the other side of the process, the proton is also treated as a system of three quarks (or a system  $q\bar{q}$  in a diquark model structure). The transition from photon to meson and the interaction with the proton occurs in the presence of a background QCD field. The Stochastic Vacuum Model [4, 5] gives a framework for this calculation and has been used with success in the study of  $J/\psi$  photo- and electroproduction processes. The calculation requires no new free parameters, incorporating the knowledge acquired in applications of hadron-hadron scattering [6], based on a functional approach [7].

These successful results give basis and justification for a practical use of simple dipole wave functions of photons and mesons and for the purely nonperturbative treatment of elastic and single diffractive meson production processes. The same framework may be used in a rather straightforward way for all vector mesons ( $\rho, \omega, \phi, \psi, \Upsilon$ ). Detailed comparison with experiments will indicate the limitations of the scheme, which in any case provides a basis upon which the role of refinements can be analysed.

A remarkable result of the treatment of  $J/\psi$  electroproduction is the factorization property [3], showing that all  $Q^2$  dependence of the amplitudes and cross sections is contained in the strength of the overlap of virtual photon and meson wave functions. The overlap strength is defined as the integral of the overlap product of wave functions, weighted with  $r^2$  ( $r$  is the dipole separation), over the light-cone coordinates of the  $q\bar{q}$  dipole.

This factorization property of the amplitude is favoured by the small size of the overlap function, which in the heavy vector meson  $J/\psi$  case is smaller than the typical range (the correlation length of the nonperturbative QCD vacuum) of the interaction with the proton.

In the cases of light vector mesons the overlap functions with real photons have rather long ranges, and the factorization property is not expected to hold for photoproduction and low  $Q^2$  processes. For electroproduction, however, as the virtuality  $Q^2$  of the photon

increases, the overlap range (as function of the dipole separation  $r$ ) decreases.

In view of the importance of this analysis for the interpretation and description of the experimental information on vector meson production, we study in this paper the properties of the photon-meson overlaps and overlap strengths for different vector mesons. We present comparison with data, mainly for electroproduction of  $\rho$  and  $J/\psi$  mesons, chosen as meaningful illustrative examples.

The description of the energy dependence requires a specific model for the coupling of  $q\bar{q}$  dipoles to the proton. In previous nonperturbative calculations of photo and electro-production of  $J/\psi$  mesons [1, 2, 3], where a quantitative description of all experimental data was envisaged, the two-pomeron model of Donnachie and Landshoff [8] was successfully employed. All QCD and hadronic parameters used in our calculation have been defined before [9]. In perturbative approaches the energy dependence is taken into account through the gluon distributions in the proton [10, 11, 12, 13]. In the elastic processes, here discussed with the purpose of pointing out specific roles of the photon and meson wave functions, the energy dependence is not very strong.

The paper is organized as follows. Sect. 2 presents the wave functions and describes their overlaps, comparing results for the  $\rho$ ,  $\omega$ ,  $\phi$ ,  $J/\psi$  and  $\Upsilon$  mesons. Weighted integrals, called overlap strengths, directly related to the amplitudes and to directly observable quantities, are evaluated and discussed in Sect. 3. In Sect. 4 examples of comparison of the predictions with the experimental data are presented. Sect. 5 summarizes predictions and results.

## II. BASIC FORMULÆ AND INGREDIENTS

For convenience we present here some basic formulae developed in our previous work on photo- and electro- production [1, 2, 3], where details can be found.

The amplitude for electroproduction of a vector meson  $V$  in polarization state  $\lambda$  is written in our framework

$$T_{\gamma^* p \rightarrow V p, \lambda}(s, t; Q^2) = \int d^2 \mathbf{R}_1 dz_1 \rho_{\gamma^* V, \lambda}(Q^2; z_1, \mathbf{R}_1) J(s, \mathbf{q}, z_1, \mathbf{R}_1) , \quad (2.1)$$

with

$$J(s, \mathbf{q}, z_1, \mathbf{R}_1) = \int d^2 \mathbf{R}_2 d^2 \mathbf{b} e^{-i\mathbf{q}\cdot\mathbf{b}} |\psi_p(\mathbf{R}_2)|^2 S(s, b, z_1, \mathbf{R}_1, z_2 = 1/2, \mathbf{R}_2) . \quad (2.2)$$

Here

$$\rho_{\gamma^* V, \lambda}(Q^2; z_1, \mathbf{R}_1) = \psi_{V\lambda}(z_1, \mathbf{R}_1)^* \psi_{\gamma^*\lambda}(Q^2; z_1, \mathbf{R}_1) \quad (2.3)$$

represents the overlap of virtual photon (virtuality  $Q^2$ ) and vector meson wave functions, and  $S(s, b, z_1, \mathbf{R}_1, 1/2, \mathbf{R}_2)$  is the scattering amplitude of two dipoles with separation vectors  $\mathbf{R}_1, \mathbf{R}_2$ , colliding with impact parameter vector  $\vec{b}$ ;  $\vec{q}$  is the momentum transfer

$$t = -\mathbf{q}^2 - m_p^2(Q^2 + M_V^2)/s^2 + O(s^{-3}) \approx -\mathbf{q}^2. \quad (2.4)$$

The differential cross section is given by

$$\frac{d\sigma}{dt} = \frac{1}{16\pi s^2} |T|^2. \quad (2.5)$$

The form of overlap written in eq.(2.3) corresponds to SCHC (s-channel helicity conservation); generalizations can be made introducing a matrix in the polarization indices. For the proton structure we adopt a simple diquark model.

The construction of the wave functions is made in a reference frame where the vector meson is essentially at rest, and we therefore use light-cone coordinates [14, 15, 16, 17, 18, 19]. The degrees of freedom for the dipole pair are the  $q \rightarrow \bar{q}$  vector in the transverse plane  $\mathbf{r} = (r \cos \theta, r \sin \theta)$ , and the momentum fractions  $z$  of the quark and  $\bar{z} = (1 - z)$  of the antiquark.

The light cone wave functions of the photon and vector meson have been discussed extensively in ([2]), where it has been shown that the physical results obtained for  $J/\psi$  photoproduction with two different forms of the meson wave function are very similar.

## Photon wave functions

The  $q\bar{q}$  wave function of the photon carries as labels the virtuality  $Q^2$  and the polarization state  $\lambda$ . The  $q\bar{q}$  state is in a configuration with given flavour  $(f, \bar{f})$  and helicities  $(h, \bar{h})$ . The colour part of the wave function leads to an overall multiplicative factor  $\sqrt{N_c}$ . The helicity and spatial configuration part of  $\psi_{\gamma^*, \lambda}(Q^2; z, r, \theta)$  is calculated in light-cone perturbation theory. The photon couples to the electric charge of the quark-antiquark pair with  $e_f \delta_{f\bar{f}}$ , where  $e_f = \hat{e}_f \sqrt{4\pi\alpha}$  and  $\hat{e}_f$  is the quark charge in units of the elementary charge for each flavour. In lowest order perturbation theory, for each polarization  $\lambda$  and flavour  $f$  content, we write [1, 2, 3, 10, 15, 20],

$$\begin{aligned} \psi_{\gamma^*, +1}(Q^2; z, r, \theta) = & \hat{e}_f \frac{\sqrt{6\alpha}}{2\pi} \left[ i\epsilon_f e^{i\theta} (z\delta_{h,+}\delta_{\bar{h},-} - \bar{z}\delta_{h,-}\delta_{\bar{h},+}) K_1(\epsilon_f r) \right. \\ & \left. + m_f \delta_{h,+}\delta_{\bar{h},+} K_0(\epsilon_f r) \right], \end{aligned} \quad (2.6)$$

$$\begin{aligned}\psi_{\gamma^*, -1}(Q^2; z, r, \theta) = & \hat{e}_f \frac{\sqrt{6\alpha}}{2\pi} \left[ i\epsilon_f e^{-i\theta} (\bar{z}\delta_{h,+}\delta_{\bar{h},-} - z\delta_{h,-}\delta_{\bar{h},+}) K_1(\epsilon_f r) \right. \\ & \left. + m_f \delta_{h,-}\delta_{\bar{h},-} K_0(\epsilon_f r) \right]\end{aligned}\quad (2.7)$$

and

$$\psi_{\gamma^*, 0}(Q^2; z, r) = \hat{e}_f \frac{\sqrt{3\alpha}}{2\pi} (-2z\bar{z}) \delta_{h,-\bar{h}} Q K_0(\epsilon_f r), \quad (2.8)$$

where

$$\epsilon_f = \sqrt{z(1-z)Q^2 + m_f^2}, \quad (2.9)$$

$\alpha = 1/137.036$ ,  $m_f$  is the current quark mass (our standard values are  $m_u = m_d = 0.2$ ,  $m_s = 0.3$ ,  $m_c = 1.25$  and  $m_b = 4.2$  GeV), and  $K_0$ ,  $K_1$  are the modified Bessel functions.

### Vector meson wave functions

The flavour dependence of the  $\rho(770)$ ,  $\omega(782)$ ,  $\phi(1020)$ ,  $J/\psi(1S)$  and  $\Upsilon(1S)$  mesons are, respectively,  $(u\bar{u} - d\bar{d})/\sqrt{2}$  (isospin 1),  $(u\bar{u} + d\bar{d})/\sqrt{2}$  (isospin 0),  $s\bar{s}$ ,  $c\bar{c}$  and  $b\bar{b}$ . We take the spin structure determined by the vector current, with expressions similar to those of the photon [1, 2, 20, 21]. We thus write

$$\begin{aligned}\psi_{V,+1}(z, r, \theta) = & \left( -ie^{i\theta} \partial_r (z\delta_{h,+}\delta_{\bar{h},-} - \bar{z}\delta_{h,-}\delta_{\bar{h},+}) \right. \\ & \left. + m_f \delta_{h,+}\delta_{\bar{h},+} \right) \phi_V(z, r), \\ \psi_{V,-1}(z, r, \theta) = & \left( -ie^{-i\theta} \partial_r (\bar{z}\delta_{h,+}\delta_{\bar{h},-} - z\delta_{h,-}\delta_{\bar{h},+}) \right. \\ & \left. + m_f \delta_{h,-}\delta_{\bar{h},-} \right) \phi_V(z, r)\end{aligned}\quad (2.10)$$

and

$$\psi_{V,0}(z, r) = (\omega 4z\bar{z}\delta_{h,-\bar{h}}) \phi_V(z, r). \quad (2.11)$$

Here  $\lambda = \pm 1$  and 0 denote transverse and longitudinal polarizations of the vector meson,  $h$  and  $\bar{h}$  represent the helicities of quark and antiquark respectively and  $m_f$  is the quark current mass. The scalar function  $\phi_V(z, r)$  contains two parameters,  $N$  and  $\omega$ , which have different values for transverse and longitudinal states; they are determined by the normalization condition and the leptonic decay width [1, 2, 3]. The parameter  $\omega$  controls the size of the hadron.

We consider two different functional forms for  $\phi_V(z, r)$ . One is given by the solution of the relativistic equation representing two particles confined by an oscillator potential. This problem admits a null plane Hamiltonian description [22] and we write

$$\phi_{BSW}(z, r) = \frac{N}{\sqrt{4\pi}} \sqrt{z\bar{z}} \exp \left[ -\frac{M_V^2}{2\omega^2} (z - \frac{1}{2})^2 \right] \exp \left[ -\frac{1}{2} \omega^2 r^2 \right], \quad (2.12)$$

which corresponds to the Bauer-Stech-Wirbel (BSW) prescription [23]. Here  $M_V$  represents the vector meson mass.

The second functional form follows the Brodsky-Lepage (BL) prescription [17, 19] for the construction of a light-cone wave function from a non-relativistic one. We here write

$$\phi_{BL}(z, r) = \frac{N}{\sqrt{4\pi}} \exp \left[ -\frac{m_f^2(z - \frac{1}{2})^2}{2z\bar{z}\omega^2} \right] \exp[-2z\bar{z}\omega^2 r^2]. \quad (2.13)$$

The experimental data for the S-wave vector mesons [24] are shown in Table I.

TABLE I: S-wave vector meson data. The coupling  $f_V$  and the electromagnetic decay width  $\Gamma_{e^+e^-}$  are related through  $f_V^2 = (3M_V\Gamma_{e^+e^-})/(4\pi\alpha^2)$ . The quantity  $\hat{e}_V$  is the effective quark charge in units of the elementary charge, determined by the  $q\bar{q}$  structure of each meson.

Meson	$M_V$ (MeV)	$\hat{e}_V$	$\Gamma_{e^+e^-}$ (keV)	$f_V$ (GeV)
$\rho(770)$	$775.9 \pm 0.5$	$1/\sqrt{2}$	$6.77 \pm 0.32$	$0.15346 \pm 0.0037$
$\omega(782)$	$782.57 \pm 0.12$	$1/3\sqrt{2}$	$0.60 \pm 0.02$	$0.04588 \pm 0.0008$
$\phi(1020)$	$1019.456 \pm 0.020$	$-1/3$	$1.261 \pm 0.03$	$0.07592 \pm 0.0018$
$J/\psi(1S)$	$3096.87 \pm 0.04$	$2/3$	$5.14 \pm 0.31$	$0.26714 \pm 0.0081$
$\Upsilon(1S)$	$9460.30 \pm 0.26$	$-1/3$	$1.314 \pm 0.029$	$0.23607 \pm 0.0026$

Values obtained for the parameters  $\omega$  and  $N$  for the two types of wave function, for transverse and longitudinal polarizations, are given in Table II.

TABLE II: Parameters of the vector meson wave functions

	BSW				BL			
	transverse		longitudinal		transverse		longitudinal	
	$\omega$ (GeV)	$N$						
$\rho(770)$	0.2159	5.2082	0.3318	4.4794	0.2778	2.0766	0.3434	1.8399
$\omega(782)$	0.2084	5.1770	0.3033	4.5451	0.2618	2.0469	0.3088	1.8605
$\phi(1020)$	0.2568	4.6315	0.3549	4.6153	0.3113	1.9189	0.3642	1.9201
$J/\psi(1S)$	0.5770	3.1574	0.6759	5.1395	0.6299	1.4599	0.6980	2.3002
$\Upsilon(1S)$	1.2850	2.4821	1.3582	5.9416	1.3250	1.1781	1.3742	2.7779

## Overlap functions

After summation over helicity indices, the overlaps of the photon and vector meson wave functions that appear in eqs.(2.1) and (2.3) are given by

$$\begin{aligned}\rho_{\gamma^*V,\pm 1;BSW}(Q^2; z, r) &= \hat{e}_V \frac{\sqrt{6\alpha}}{2\pi} \left( \epsilon_f \omega^2 r [z^2 + \bar{z}^2] K_1(\epsilon_f r) + m_f^2 K_0(\epsilon_f r) \right) \phi_{BSW}(z, r) \\ &\equiv \hat{e}_V \hat{\rho}_{\gamma^*,\pm 1;BSW}(Q^2; z, r)\end{aligned}\quad (2.14)$$

and

$$\begin{aligned}\rho_{\gamma^*V,\pm 1;BL}(Q^2; z, r) &= \hat{e}_V \frac{\sqrt{6\alpha}}{2\pi} \left( 4\epsilon_f \omega^2 r z \bar{z} [z^2 + \bar{z}^2] K_1(\epsilon_f r) + m_f^2 K_0(\epsilon_f r) \right) \phi_{BL}(z, r) \\ &\equiv \hat{e}_V \hat{\rho}_{\gamma^*,\pm 1;BL}(Q^2; z, r)\end{aligned}\quad (2.15)$$

for the transverse case, BSW and BL wave functions respectively. Here  $\hat{e}_V$  is as given in Table I. For the longitudinal case we can write jointly

$$\rho_{\gamma^*V,0;X}(Q^2; z, r) = -16\hat{e}_V \frac{\sqrt{3\alpha}}{2\pi} \omega z^2 \bar{z}^2 Q K_0(\epsilon_f r) \phi_X(z, r) \equiv \hat{e}_V \hat{\rho}_{\gamma^*,0;X}(Q^2; z, r) \quad (2.16)$$

where  $X$  in the index stands for BSW or BL.

For real photon-vector meson overlap,  $Q = 0$ , the longitudinal part vanishes and  $\epsilon_f \rightarrow m_f$ .

The ranges (in the  $r$  variable) of the photon-meson overlap functions are crucial in the factorization process that allows to write the amplitude with a factor containing all  $Q^2$  dependence of the amplitude. We may characterize these ranges through the values  $r_{\text{peak}}$  of the variable  $r$  where the overlap weights  $2\pi r \int \rho(Q^2; z, r) dz$  have their maxima.

In Fig. 1 the results of numerical calculations for the peak positions  $r_{\text{peak}}$  are shown, as functions of  $Q^2$ , for all vector mesons. These results are very nearly the same for both kinds of wave functions, so that we show graphs for BSW only. The plot using the variable  $Q^2 + M_V^2$  exhibits the impressive universality of the functions describing the peaks of the longitudinal case.

All figures are represented by the form

$$r_{\text{peak}} = \frac{A_{\text{peak}}}{\sqrt{Q^2 + M_V^2}} , \quad (2.17)$$

with the values of (dimensionless)  $A_{\text{peak}}$  given in Table III.

Since it has been shown [3] that the  $J/\psi$  photo- and electroproduction processes are well described by factorized amplitudes, values of  $r_{\text{peak}}$  smaller than  $0.4 \text{ GeV}^{-1}$  should guarantee that the overlap extensions are small enough for factorization. Thus in the case of the  $\rho$  meson electroproduction  $Q^2$  must be larger than  $10 \text{ GeV}^2$  for longitudinal and

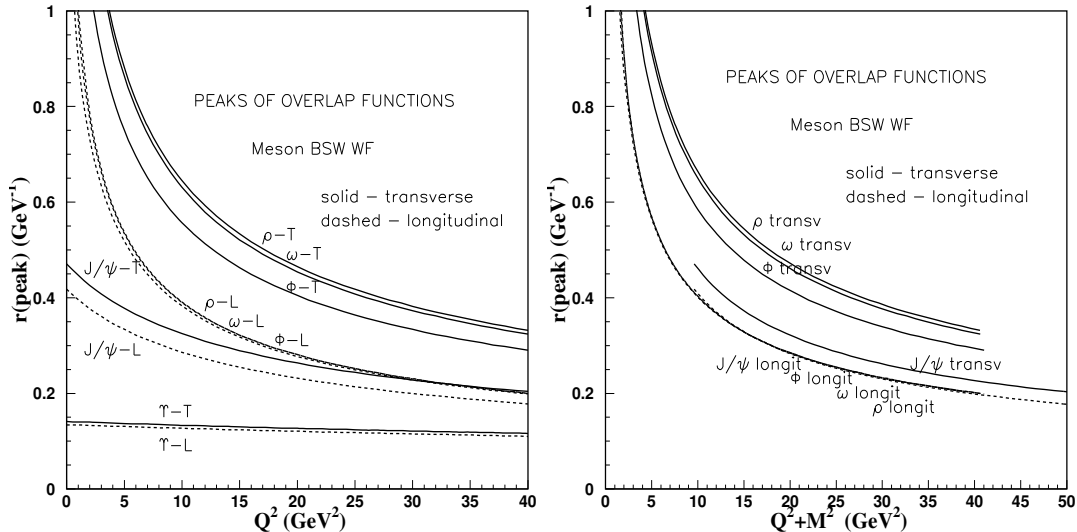


FIG. 1: Positions  $r_{\text{peak}}$  of the maximum values of the density weights  $2\pi r \int \rho(Q^2; z, r) dz$  of the photon-meson overlap functions for all vector mesons. These quantities inform about the extension of the region where photon-meson transition occurs, and are related to description of the  $Q^2$  dependence of the amplitudes in terms of overlap functions. The figure shows values for the BSW wave functions; those for BL are very similar. All lines have the form  $r_{\text{peak}} = A_{\text{peak}} / \sqrt{Q^2 + M^2}$ , with impressive universality in the longitudinal case (same value of  $A_{\text{peak}}$  for all mesons, as shown in Table III) and regular displacements in the transverse case.

TABLE III: Parameter  $A_{\text{peak}}$  of eq. (2.17).

Meson	$\rho$	$\omega$	$\phi$	$\psi$	$\Upsilon$
BSW transverse	2.10	2.06	1.85	1.44	1.33
BSW longitudinal	1.27	1.28	1.27	1.26	1.26
BL transverse	2.22	2.17	1.93	1.44	1.33
BL longitudinal	1.29	1.30	1.29	1.27	1.26

larger than  $20 \text{ GeV}^2$  for transverse polarizations. Actually, since for  $Q^2 \gtrsim 10 \text{ GeV}^2$  the longitudinal contribution is dominant, factorization in the elastic cross section (longitudinal plus transverse) for  $\rho$  electroproduction is valid for all  $Q^2$  above  $10 \text{ GeV}^2$ . This is true except for the ratio  $R = \sigma(L)/\sigma(T)$  that depends specifically on the two polarized cross sections, and where then the factorization condition requires  $Q^2 \geq 25 \text{ GeV}^2$  in  $\rho$  and  $\omega$  electroproduction.

### III. OVERLAP STRENGTHS

Previous work [3] has shown the importance for elastic electroproduction processes of the quantities called overlap strengths, formed by integration over the internal variables of the quark-antiquark pairs of the overlap function multiplied by  $r^2$ . They are written for transverse and longitudinal polarizations

$$Y_{\gamma^*V,T;X}(Q^2) = \int_0^1 dz \int d^2\mathbf{r} r^2 \rho_{\gamma^*V,\pm 1,X}(Q^2; z, r) \equiv \hat{e}_V \hat{Y}_{\gamma^*V,T;X}(Q^2) \quad (3.1)$$

and

$$Y_{\gamma^*V,L;X}(Q^2) = \int_0^1 dz \int d^2\mathbf{r} r^2 \rho_{\gamma^*V,0,X}(Q^2; z, r) \equiv \hat{e}_V \hat{Y}_{\gamma^*V,L;X}(Q^2) \quad (3.2)$$

with  $X$  for BSW or BL. These quantities appear as independent factors in the amplitude, containing all its dependence on  $Q^2$  and on the vector meson and quark masses, whenever the range of the overlap region is small compared to the typical range of the nonperturbative interaction governing the process. This simplification occurs when  $Q^2 + M_V^2 \gtrsim 10 \text{ GeV}^2$ , which means always in  $J/\psi$  and  $\Upsilon$  production, and  $Q^2 \gtrsim 10 \text{ GeV}^2$  in  $\rho, \omega$  and  $\phi$  electroproduction.

Properties of the transverse and longitudinal squared strengths and of their sums are shown in Figs. 2 and 3. Using the variable  $Q^2 + M_V^2$ , where  $M_V$  is the mass of the corresponding vector meson, and extracting factors given by the effective squares of the quark pair charges ( $\hat{e}_V^2 = 1/2, 1/18, 1/9, 4/9$  and  $1/9$  for the  $\rho, \omega, \phi, \psi$  and  $\Upsilon$  mesons respectively), universalities observed in the experimental data are exhibited.

The  $Q^2$  dependence of the squared strengths can be represented by

$$\hat{Y}_{\gamma^*V,T}^2(Q^2) = \frac{A_T}{(1 + Q^2/M_V^2)^{n_T}} , \quad (3.3)$$

and

$$\hat{Y}_{\gamma^*V,L}^2(Q^2) = \frac{A_L(Q^2/M_V^2)}{(1 + Q^2/M_V^2)^{n_L}} , \quad (3.4)$$

with the values of  $A_T$ ,  $n_T$ ,  $A_L$  and  $n_L$  given in Table IV.

The use of the numerical values  $M_V^2$  of the vector mesons masses in these parametrizations is conventional, being successful in the description of data (in rather limited  $Q^2$  intervals). The form is inspired in the Vector Dominance Model, with  $n_T = 2$  corresponding to the vector meson propagator. The parametrization given above covers a wide range in  $Q^2$ , and can be improved in the light vector mesons cases with  $M$  left as a free parameter (fitting results recommend increases by up to 30 percent in  $M_V$ ). However differences

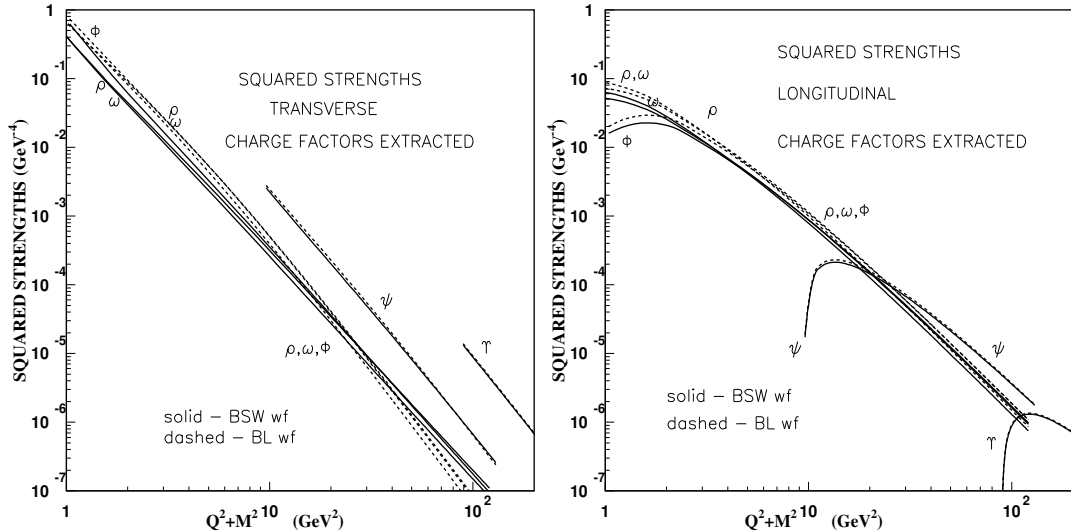


FIG. 2: Transverse and longitudinal squared overlap strengths  $\hat{Y}_{T,L}^2$  as functions  $Q^2 + M_V^2$ , where  $M_V$  is the mass of each meson. For large  $Q^2 + M_V^2$  these quantities show the shapes of the cross sections with charge factors  $\hat{e}_V^2$  extracted. For  $Q^2 \gtrsim 20 \text{ GeV}^2$  in the transverse case for light mesons the BL gives is smaller than the BSW wave function. This strongly influences the ratio of longitudinal to transverse cross sections, and can be tested experimentally. The squared strengths have the forms  $A_T/(1 + Q^2/M_V^2)^{n_T}$  and  $A_L(Q^2/M_V^2)/(1 + Q^2/M_V^2)^{n_L}$ , with parameters given in Table IV.

TABLE IV: Parameters  $A_T$ ,  $n_T$ ,  $A_L$  and  $n_L$  of eqs. (3.3), (3.4) for the squared overlap strengths  $\hat{Y}^2$  in  $\text{GeV}^{-4}$ . These quantities are directly related to the cross sections.

Meson	$\rho$	$\omega$	$\phi$	$\psi$	$\Upsilon$					
Parameter	$A_{T/L}$	$n_{T/L}$	$A_{T/L}$	$n_{T/L}$	$A_{T/L}$	$n_{T/L}$	$A_{T,L}$	$n_{T/L}$		
BSW transv	2.18	3.16	2.11	3.23	0.57	3.27	0.26E(-2)	3.48	1.33E(-5)	3.68
BSW longit	0.58	3.38	0.74	3.50	0.23	3.49	0.19E(-2)	3.63	1.14E(-5)	3.73
BL transv	4.46	3.35	4.63	3.45	1.08	3.47	0.30E(-2)	3.51	1.39E(-5)	3.68
BL longit	0.84	3.42	1.04	3.54	0.32	3.53	0.21E(-2)	3.66	1.18E(-5)	3.73

are small and not important at the moment, in view of the limited data. In any case, the reason for the appealing and efficient parametrizations of the form  $1/(Q^2 + M_V^2)^n$  is not understood.

Fig. 4 shows the ratios of squared strengths of the longitudinal and transverse cases, for the different vector mesons. According to the factorization property, these quantities

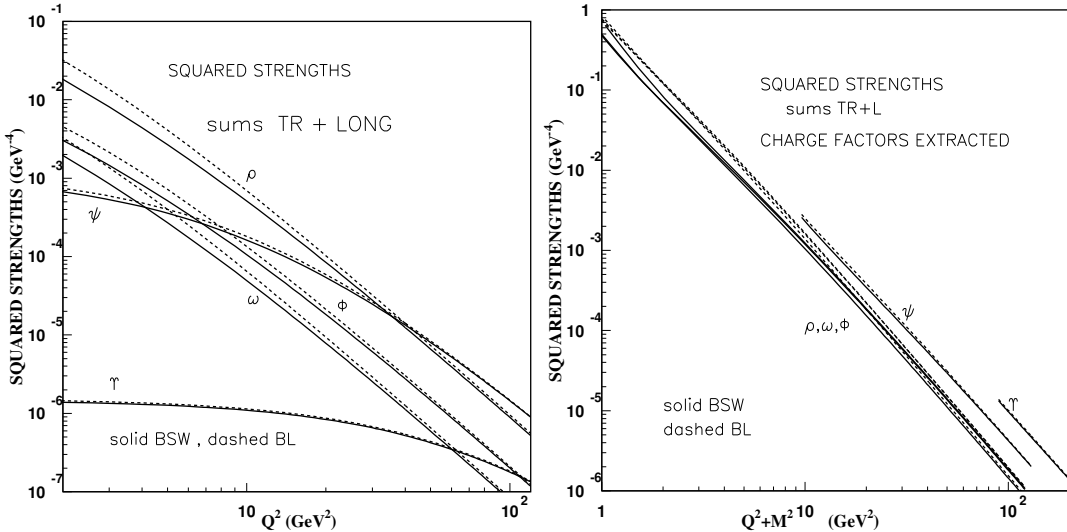


FIG. 3: Sums of transverse and longitudinal squared strengths. These quantities give all  $Q^2$  dependence of the integrated elastic cross sections. In the right hand side the same quantities, with extraction of charge factors  $\hat{e}_V^2$ , as functions of  $Q^2 + M_V^2$ . Due to the nearly linear behaviour in the log-log scale, the sums of squared strengths can be parametrized with forms  $A/(Q^2 + M_V^2)^n$ .

correspond to the ratios of longitudinal and transverse cross sections, which are observed experimentally. For light vector mesons ( $\rho, \omega, \phi$ ) the value of  $Q^2$  must be large enough, namely  $Q^2 + M_V^2 \gtrsim 20 \text{ GeV}^2$  and we observe that for these mesons the BSW and BL wave functions show different behaviour in the  $Q^2$  dependence.

In studies of the forward photoproduction of vector mesons the amplitude has been written in a factorized form (see eq. (5) in the second paper of ref. [25])

$$M(VN, \mathbf{q} = 0) = \langle V | \sigma(r) | \gamma^* \rangle = \int_0^1 dz \int d^2 \mathbf{r} \sigma(r) \Psi_V(r, z)^* \Psi_{\gamma^*}(r, z), \quad (3.5)$$

where  $\sigma(r)$  is the cross section for a dipole of separation  $\mathbf{r}$  with the nucleon, which for small  $r$  has the form  $\sigma(r) \propto r^2$ . This leads to amplitude with forms similar to the overlap strengths of eqs. (3.1,3.2). Without assuming specific forms for the vector meson wave functions, but considering that the vector meson sizes are large and their structures do not depend strongly on  $r$  in the most relevant range for the interaction with the proton, an estimate is made for the peak values of the integrand in the amplitude. With the photon represented by the asymptotic form  $\exp(-\epsilon r)$ , taking a non-relativistic extreme  $M_V = 2m_f$  and fixing  $z = 1/2$ , the density  $2\pi r \exp(-\epsilon r)$  has a peak at  $r_Q = 2/\sqrt{Q^2 + M_V^2}$ . This expression must be compared with eq. (2.17) and the parameter values given in Table III. With the QCD dependence  $\sigma(r) \propto r^2$  of the dipole cross section for small  $r$ , the integrand in the amplitude (3.5) has a peak at  $r_s = C_s/\sqrt{Q^2 + M_V^2}$ , with  $C_s = 6$ . This

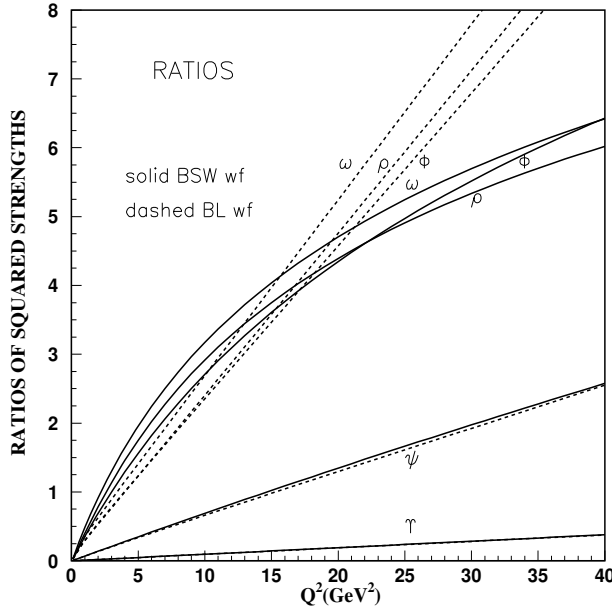


FIG. 4: Ratios of longitudinal to transverse squared strengths, for different vector mesons. In the cases of light vector mesons ( $\rho, \omega, \phi$ ) the BSW and BL wave functions show different behaviour in the  $Q^2$  dependence.

is called *scanning* radius, to convey the idea that at this value occur the most important contributions to the integrand, so that the measurements of the amplitude in photoproduction inform directly [26] about the value of the vector meson wave function at  $r = r_s$ . With our explicit forms of wave function for the vector mesons, the integrands in the overlap strengths in eqs. (3.1,3.2), after  $z$  integration, inform the positions of the peak values of the contributions for all vector mesons, for transverse and longitudinal polarizations. Putting the results in the same parametrized form, we obtain for the  $J/\psi$  meson  $C_s = 5.4$  and  $4.7$  respectively for transverse and longitudinal polarizations. However this is not an accurate parametrization, and we obtain much better representations with the forms  $3.8/(Q^2 + M_V^2)^{0.4}$  and  $3.4/(Q^2 + M_V^2)^{0.4}$  for the transverse and longitudinal cases respectively, or alternatively with the forms where the mass values are modified, namely  $6.0/\sqrt{Q^2 + (3.92)^2}$  and  $5.3/\sqrt{Q^2 + (3.92)^2}$ . We notice that in all cases the ratio of longitudinal over transverse radii is about  $0.88$ . We must remark however that the shapes of the integrands (after  $z$  integration) as functions of  $r$  are rather broad, so that fixing a value  $r = r_s$ , whatever the expression for  $r_s$ , cannot give accurate information on details of the meson wave function. This remark is particularly meaningful since we show that with our models for the wave functions we obtain good description of the data [1, 2, 3]. Actually, evaluation of observables in photoproduction and electroproduction processes

seem to depend only weakly of the form of the vector meson wave function [27].

#### IV. EXPERIMENTAL DATA

The factorization property means that we may write

$$T_{\gamma^* p \rightarrow Vp, T/L}(s, t; Q^2) \approx (-2is) G(t) Y_{\gamma^* V, T/L; X}(Q^2) \quad (4.1)$$

with  $Y$  given by eqs. (3.1), (3.2).  $G(t)$  depends on the specific framework and model for the dipole-dipole interaction and on the proton wave function. Depending on the dynamical structure of the model, it may also contain energy dependence due to the dipole-dipole interaction.

The energy dependence in our model is motivated by the two-pomeron model of Donnachie and Landshoff [8]. For  $R_1 \leq r_c \approx 0.22$  fm the coupling through the hard pomeron induces the energy dependence  $(s/s_0)^{0.42}$ , while the coupling of large dipoles follows the soft pomeron energy dependence  $(s/s_0)^{0.0808}$ . The reference energy is  $s_0 = (20 \text{ GeV})^2$ . The numerical values for  $r_c$  and  $s_0$  are taken from [9]. We therefore split the integration over  $R_1$  appearing in eq. (2.1) and in the overlap strengths into hard ( $h$ ) and soft ( $s$ ) parts, as fully described in the studies of  $J/\psi$  photo and electroproduction [2]. We then write

$$T_{\gamma^* p \rightarrow Vp, T/L}(s, t; Q^2) \approx (-2is) G(t) \left( T_h^{T/L}(Q^2) \left( \frac{s}{s_0} \right)^{\epsilon_h} + T_s^{T/L}(Q^2) \left( \frac{s}{s_0} \right)^{\epsilon_s} \right) \quad (4.2)$$

with

$$\begin{aligned} T_h^{T/L}(Q^2) &= 2\pi \int_0^{r_c} dR_1 \int_0^1 dz_1 \left( \frac{R_1^2}{r_c^2} \right)^{\epsilon_h} R_1^3 \rho_{\gamma^*, V, T/L}(Q^2, z_1, R_1) , \\ T_s^{T/L}(Q^2) &= 2\pi \int_{r_c}^{\infty} dR_1 \int_0^1 dz_1 R_1^3 \rho_{\gamma^*, V, T/L}(Q^2, z_1, R_1) . \end{aligned} \quad (4.3)$$

The Model of the Stochastic Vacuum has been applied very successfully to the processes of photo and electroproduction of  $J/\psi$  and  $\Upsilon$  vector mesons [1, 2, 3]. All observables of differential and integrated elastic cross sections are reproduced in the calculation, without use of any new external parameter. In Fig. 5 we show the  $Q^2$  dependence of the elastic electroproduction cross section for  $\gamma^* p \rightarrow \psi p$  obtained before [3]. The data are from HERA-ZEUS [28] and HERA-H1 [29]. The line corresponds to a constant multiplied by the squared overlap strength. The Stochastic Vacuum Model is responsible for the value of this constant number, which comes out of the calculation without any free parameter [3].

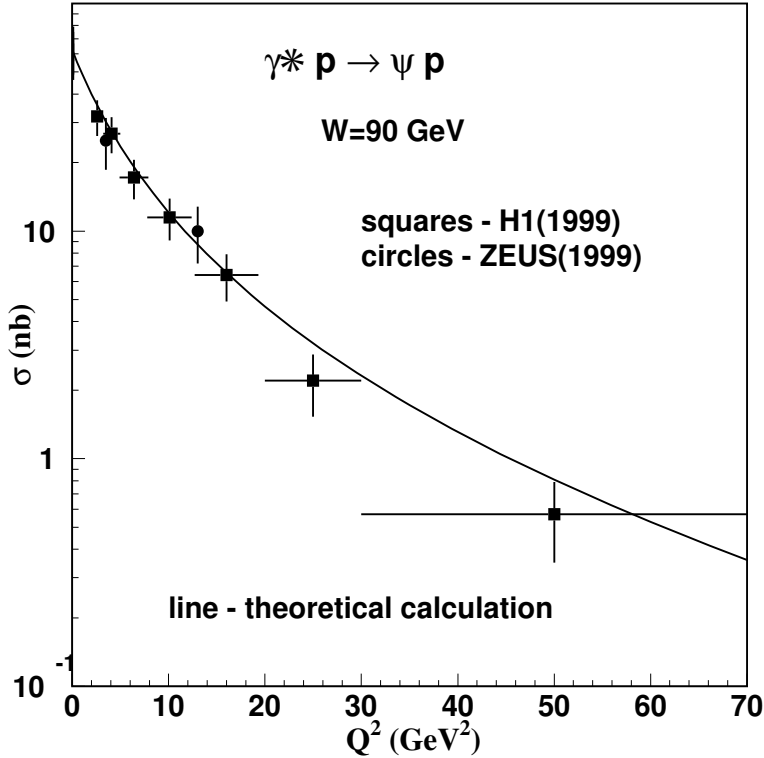


FIG. 5: Integrated elastic cross section for  $J/\psi$  electroproduction as function of  $Q^2$ . Data from [28] (circles) and [29] (squares). The line goes with the squared overlap strength, multiplied by a single constant determined without free parameter using the stochastic vacuum model [3].

These calculations have shown a property of factorization of the amplitudes, with all  $Q^2$  dependence, and all properties specifically dependent on the vector meson structure, described by the quantity called overlap strength, which is the integral over the dipole variables  $r$  and  $z$ , with a weight  $r^2$ , of the photon-meson overlap function.

Since the data on  $J/\psi$  formation has been described before, we here present results concerning mainly  $\rho$  electroproduction. Our purpose is to demonstrate the contents of information concentrated in the wave function overlaps. The message is that details of proton structure functions are not visible in the kinematical conditions where the nonperturbative method has a full control of the elastic electroproduction process.

In the examples concerning the  $\rho$  meson data presented in this section we somewhat overlook the energy dependence, which is not strong, and take as if  $s = s_0 = (20 \text{ GeV})^2$  in the data. Where ratios are concerned, the energy dependence is strongly reduced. We explain the situation in detail in each case.

Fig. 6 shows data of elastic  $\rho$  electroproduction, from Zeus [28] and H1 [30] at energies  $W = \sqrt{s} = 35 - 50 \text{ GeV}$  and  $W = 75 \text{ GeV}$  respectively. The solid line is the overlap

strength squared, multiplied by a fixed number

$$C = 74 \times 10^3$$

converting the squared strengths in  $\text{GeV}^{-4}$  to the cross section in  $\text{nb}$ . The figure shows that the  $Q^2$  dependence of the data above  $Q^2 = 10 \text{ GeV}^2$  is well represented by the overlap of photon and  $\rho$  meson wave functions. The solid and dashed lines refer to BSW and BL wave functions. Energy dependence (which is small) is not included in the calculation of these lines.

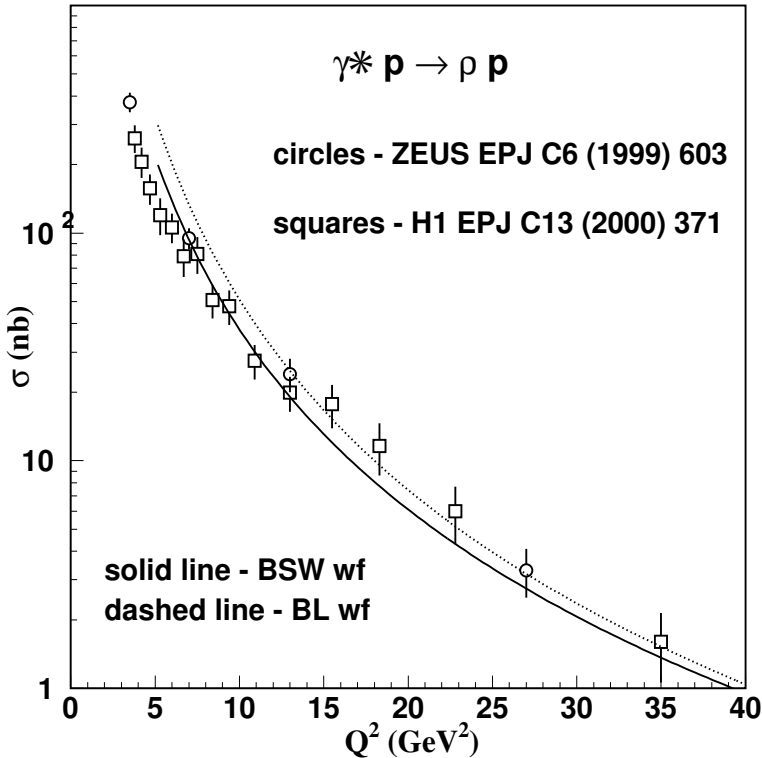


FIG. 6: Integrated elastic cross section for  $\rho$  electroproduction as a function of  $Q^2$ . Data from Zeus [28] (empty circles) and H1 [30] (empty squares). Solid and dashed lines for BSW and BL wavefunctions respectively. With parametrizations of the form  $1/(1+Q^2/M_V^2)^n$ , the theoretical lines have  $n = 2.74$  (BSW) and  $n = 2.90$  (BL).

Fig. 7 shows the cross sections for  $\rho$ ,  $\psi$  and  $\Upsilon$  electroproduction, reduced by the charge factors  $1/2$ ,  $4/9$  and  $1/9$  respectively, plotted against the variables  $Q^2 + M_V^2$ . The  $\psi$  and  $\rho$  data and theoretical lines are the same as in Figs. 5 and 6. The  $\Upsilon$  photoproduction data (triangles) from ZEUS [31] and H1 [32] at about  $W=100$  GeV are compared to the theoretical calculation at this energy [2].

The plot exhibits the partial universality of the data in terms of the variables  $Q^2 + M_V^2$ , showing that the shifts observed experimentally between the heavy and light mesons are

theoretically reproduced as natural consequences of the construction of the meson wave functions.

Our method for building the wave functions uses the experimental decay rates of the vector mesons, which effectively incorporate QCD corrections, and thus makes realistic representations of the vector meson structures. We may conjecture that the shifts observed in plots of data and of squared strengths are due to QCD corrections of the decay rates, which specifically depend on the quark masses (namely on the vector meson type), and thus are different for the different mesons.

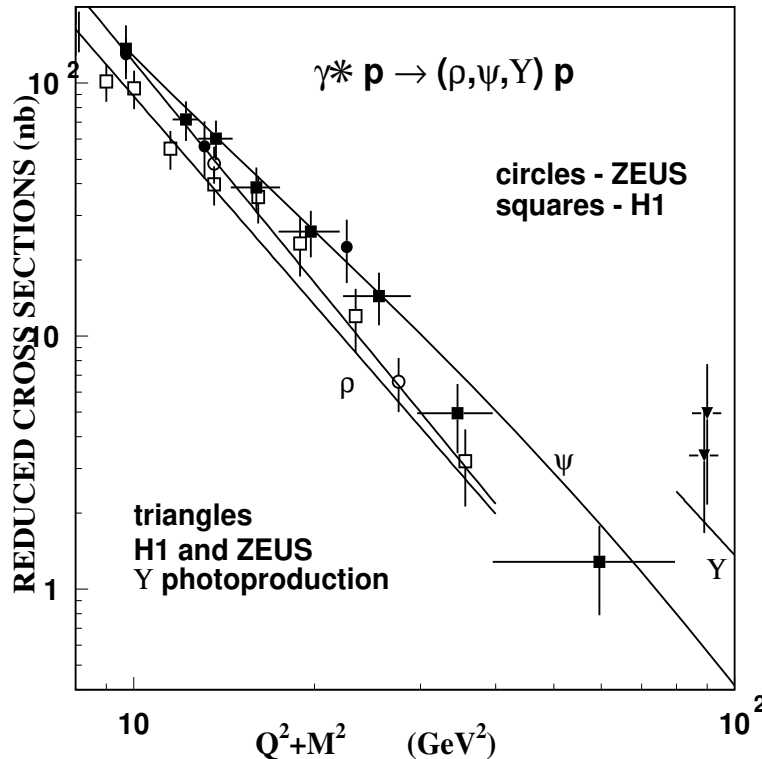


FIG. 7: Integrated elastic cross section for  $J/\psi$  [28, 29] and  $\rho$  electroproduction [28, 30], and for  $\Upsilon$  photoproduction [31, 32]. The lines represent the theoretical calculations explained in the text. The differences between the two kinds of vector meson wave function are not important, as shown in Fig. 3.

Fig. 8 shows the experimental ratio [28, 30, 33, 34] between longitudinal and transverse cross sections in  $\rho$  electroproduction, compared to the ratio of longitudinal to transverse squared overlap strengths. In the ratio, the specific dynamics of the process of interaction of the  $q - \bar{q}$  dipoles with the proton cancels out, so that a clear view is obtained of the self-contained role of the photon-meson wave function overlap. The comparison is to be taken more seriously for  $Q^2 \gtrsim 10 \text{ GeV}^2$ . The cross section with transverse polarization

falls to zero much more quickly, and the ratio  $R = \sigma(L)/\sigma(T)$  becomes sensitive to the helicity structure of the wave function. Thus the predictions for the ratio  $R$  given by the BSW and BL wave functions, in the light meson cases, are very different. This is obviously an area that deserves exploration, both experimentally and theoretically.

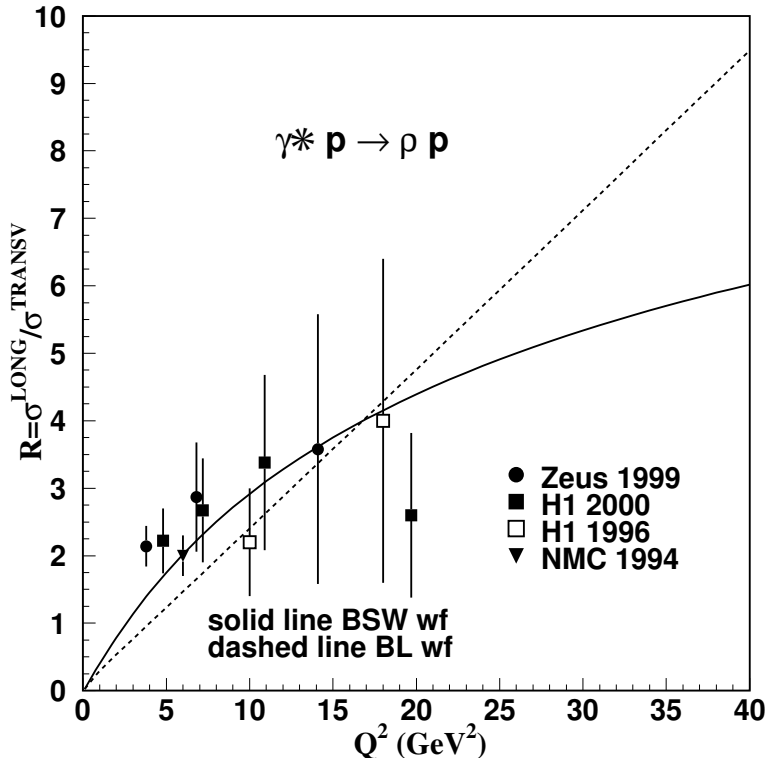


FIG. 8: Ratio of cross sections with longitudinal and transverse polarisations in  $\rho$  electroproduction. Data from [28, 30, 33, 34]. The lines represent ratios of overlap strengths. The ratios calculated with BSW and BL wavefunctions become dramatically different for large  $Q^2$ .

Under the conditions of factorization in the amplitudes, ratios of electroproduction cross sections for different vector mesons cancel factors connected to the proton structure and to the dipole-proton interaction (which in the case of the Stochastic Vacuum Model is determined by the mechanism of vacuum correlations). These ratios are then explicitly and simply determined by ratios of squared overlap strengths. Fig. 9 gives our predictions for the ratios of  $\psi$  to  $\rho$  cross sections, together with the published data [28]. There are some preliminary data presented in conferences by Zeus and H1. We warn that these ratios are delicate, because of the strong  $Q^2$  dependence of the cross sections. Ratios must be formed with cross sections measured at precisely the same  $Q^2$ , and preferably by the same experiment, in order to take advantage of cancellation of systematic uncertainties.

The experimental data on  $J/\psi$  electroproduction mentioned in this paper are confirmed

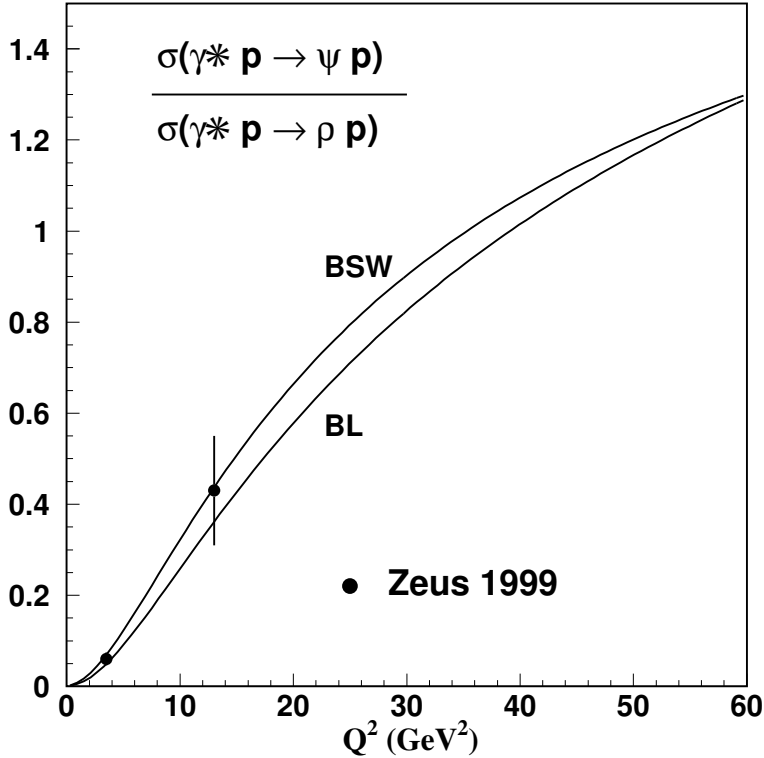


FIG. 9: Ratio of cross sections for electroproduction of  $J/\psi$  and  $\rho$  mesons. Data from Zeus [28]. Lines represent ratios of overlap strengths for  $J/\psi$  and  $\rho$  mesons using two kinds of wave function (BSW and BL, explained in the text.)

by the ZEUS data recently published [35].

## V. CONCLUSIONS

The results discussed in this paper are consequences of the form of the amplitude in eqs. 2.1, 2.2, 2.3 written as integrations over configuration space coordinates. The fundamental quantity in the calculations is the dipole-dipole interaction, which in nonperturbative language takes the form of loop-loop correlation in QCD vacuum. The dipoles appear in the  $\gamma^* - V$  transition (overlap of the wave functions) and in the proton structure. The treatment is typical of soft QCD calculation, and provides very successful phenomenology of pp and hadron-hadron scattering [6].

The Model of the Stochastic Vacuum leads to a specific calculation of the loop-loop interaction, reducing the determination of all observables to two universal QCD parameters (the gluon condensate and the correlation length). In our calculation the MSV provides a single number, relating the overlap strength squared to the cross section. All observables,

including polarization and  $t$ -momentum transfer dependences, are predicted uniquely, without free parameters.

In the treatment of  $J/\psi$  electroproduction we have shown that, where the range of the overlap function is small compared to the proton size and to the range of correlation functions of the QCD vacuum, a factorization of the amplitude takes place [3], such that the  $Q^2$  dependence of observables is fully described in terms of the overlap strengths of eqs.3.1. For heavy, small sized vector mesons (such as  $J/\psi$ ), factorization of the amplitude occurs even in photoproduction processes. For the light vector mesons, of broader wave functions and broader overlaps with the photon when  $Q^2$  is small, the factorization holds clearly only for large values of  $Q^2$ . In  $\rho$  electroproduction this means  $Q^2 \gtrsim 10 \text{ GeV}^2$ .

In Figs. 5 and 6 we compare our results with experimental data on the integrated cross sections for  $J/\psi$  and  $\rho$  electroproduction. Fig. 7, in which cross sections are plotted against  $Q^2 + M_V^2$  shows the almost universal behaviour of different vector mesons, with the shift that has been observed experimentally and that is here quantitatively predicted by the overlap of wave functions.

Fig. 4, with the ratio of longitudinal to transverse cross sections, fully evaluated through ratios of the corresponding squared overlap strengths, is beautifully confirmed experimentally by figure 5 in [3] for  $J/\psi$  and in Fig. 8 for  $\rho$  electroproduction.

Fig. 9 shows again in an absolutely clear form the role of the factorization property: the ratios of cross sections for different vector mesons are fully determined by the ratios of their squared overlap strengths.

### Acknowledgments

The authors are grateful to H. G. Dosch for participating in several aspects of the present work, and wish to thank DAAD(Germany), CNPq(Brazil), CAPES(Brazil) and FAPERJ(Brazil) for support of the scientific collaboration program between Heidelberg, Frankfurt and Rio de Janeiro groups working on hadronic physics.

---

- [1] H.G. Dosch, T. Gousset, G. Kulzinger and J.J. Pirner, Phys. Rev. D **55** (1997) 2602.
- [2] H.G. Dosch and E. Ferreira, Eur. Phys. J. C **29**, 45 (2003).

- [3] H.G. Dosch and E. Ferreira, Phys. Lett. B **576**, 83 (2003).
- [4] H.G. Dosch, Phys. Lett. B **190** (1987) 177.
- [5] H.G. Dosch and Y.A. Simonov, Phys. Lett. B **205** (1988) 339.
- [6] H.G. Dosch, E. Ferreira and A. Kramer, Phys. Rev. D **50** (1994) 1992.
- [7] O. Nachtmann, Ann. Phys. **209**, 436 (1991).
- [8] A. Donnachie and P.V. Landshoff, Phys. Lett. B **437** (1998) 408.
- [9] A. Donnachie and H. G. Dosch, Phys. Rev. D **65** (2002) 014019.
- [10] S.J. Brodsky, L. Frankfurt, J.F. Gunion, A.H. Mueller, M. Strikman, Phys. Rev. D **50**, 3134 (1994).
- [11] A.H. Mueller, Nucl. Phys. B **415**, 373 (1994).
- [12] A.D. Martin, M.G. Ryskyn and T. Teubner, Phys. Rev. **D62**, 014022 (2000).
- [13] A.H. Mueller, Nucl. Phys. **B643**, 501 (2002).
- [14] P.A.M. Dirac, Rev. Mod. Phys. **21**, 392 (1949).
- [15] J.B. Kogut and D. E. Soper, Phys. Rev. **D1**, 2910 (1970); J.D. Bjorken, J.B. Kogut and D.E. Soper, Phys. Rev. **D3**, 1382 (1971).
- [16] J. Kogut, L. Susskind, Phys. Rep. **8**, 75 (1973).
- [17] G.P. Lepage and S.J. Brodsky, Phys. Rev. **D22**, 2157 (1980).
- [18] G.P. Lepage *et al.*, in *Particles and Fields 2*, Proceedings of the Banff Summer Institute, Banff, Canada, 1981, edited by A.Z. Capri and A.N. Kamal (Plenum, New York, 1983).
- [19] S.J. Brodsky, H.C. Pauli and S.S. Pinsky, Phys. Rep. **301**, 299 (1998).
- [20] N. N. Nikolaev and B. G. Zakharov, Z. Phys. **C49**, 607 (1991).
- [21] A. C. Caldwell and M. A. Soares, Nucl. Phys. **A696**, 125 (2001).
- [22] H. Leutwyler, Ann. Phys. **112**, 94 (1978).
- [23] M. Wirbel, B. Stech and M. Bauer, Z. Phys. **C29**, 637 (1985) ; M. Bauer, B. Stech and M. Wirbel, Z. Phys. C **34** (1987) 103.
- [24] K. Hagiwara *et al.*, Phys. Rev. **D66**, 010001 (2002) and update in <http://pdg.lbl.gov>
- [25] B.Z. Kopeliovich, J. Nemchik, N.N. Nikolaev and B.G. Zakharov, Phys. Lett. **B309**, 179 (1993); B.Z. Kopeliovich, J. Nemchik, N.N. Nikolaev and B.G. Zakharov, Phys. Lett. **B324**, 469 (1994).
- [26] J. Nemchik, N.N. Nikolaev and B.G. Zakharov, Phys. Lett. **B341**, 228 (1994); J. Nemchik, N.N. Nikolaev, E. Predazzi and B.G. Zakharov, Z. Phys. **C75**, 71 (1997).
- [27] S. Munier, A.M. Staśto, A.H. Mueller, Nucl. Phys. **B603**, 427 (2001).
- [28] J. Breitweg *et al.*, Zeus Coll., Eur. Phys. J. C **6** (1999) 603.

- [29] C. Adloff et al., H1 Coll. Eur. Phys. J. C **10** (1999) 373.
- [30] C. Adloff et al., H1 Coll. Eur. Phys. J. C **13** (2000) 371.
- [31] J. Breitweg et al., Zeus Coll., Phys. Lett. B **437** (1998) 432.
- [32] C. Adloff et al., H1 Coll. Phys. Lett. B **483** (2000) 23.
- [33] S. Aid et al, H1 Coll., Nucl. Phys. B bf 468 (1996) 3.
- [34] M. Arneodo et al., NMC Coll., Nucl. Phys. B **429** (1994) 503 ; P. Amaudruz et al., Zeit. Phys. C **54** (1992) 239.
- [35] S. Chekanov et al., ZEUS Coll., Nucl. Phys. B **695** (2004) 3.